28

FPRINT-94-21

Proposal

Search for Direct CP-Violation in Charged $K \to 3\pi$ Decays at the IHEP 70 GeV Accelerator

by

The Tagged-Neutrino Collaboration

Proposal

Search for Direct CP-Violation in Charged $K \longrightarrow 3\pi$ Decays at the IHEP 70 GeV Accelerator

(Tagged-Neutrino Collaboration)

A.Bel'kov, E.Belyakova, M.Bondila, D.Gavrischuk, A.Feschenko, G.Jarygin, M.Kadykov, V.Kukhtin, V.Odintsov, A.Pose, D.Pose, S.Plyashkevich, I.Savin, G.Shabratova

JINR Dubna, Russia

V.Anykeyev, S.Belikov, S.Denisov, A.Dushkin, N.Fedjakin, A.Galyaev, J.Gilitsky, S.Gurdjiev, V.Kochetkov, T.Koroleva, I.Kotov, A.Kozelov, V.Kurbakov, A.Lanyov, V.Lipajev, I.Mandjavidze, S.Medved, V.Mikhailin, J.Mikhailov, S.Mukhin, V.Onuchin, J.Pistchalnikov, A.Schukin, I.Shein, A.Soldatov, A.Spiridonov, A.Starkov, A.Vasilyev, V.Zhigunov

IHEP Protvino, Russia

V.Genchev, V.Krasteva

INRNE Sofia, Bulgaria
—, Inst. Nucl. Res.

J.Bähr, G.Bohm, L.Kaschluhn, A.Schaale, A.Schwind

DESY Zeuthen, Germany
DESY-IFH,

Contents

I. Introduction

The idea to investigate rare K decays and especially the question of direct CP violation at the tagged-neutrino facility for the U-70 accelerator of the IHEP Serpukhov dates back to the first versions of the proposal for that facility [1]. After some theoretical work [2] a very promising possibility was found for checking direct CP-violation in a context different from the neutral K-system and therefore -in case of a positive result- clearly contradicting the superweak model [5]. Some preliminary estimates have been given in [3]. The main idea consists in the precision measurement of the charge asymmetry of the Dalitz-plot slopes for $K^{\pm}\to\pi^{\pm}\pi^0\pi^0$ decays.

As many important questions were left open in the above mentioned paper [3], and several new aspects appeared during the completions of the apparatus, we present here a new proposal restricted to this topic, leaving all other experimental work at the Tagged-Neutrino Facility untouched.

The possibility to check slope coefficients $g_{\tau,\tau'}$ in $K^{\pm}_{\tau}$ and $K^{\pm}_{\tau'}$ decays ($K^{\pm}\to\pi^{\pm}\pi^{+}\pi^{-}$, $K^{\pm}\to\pi^{\pm}\pi^0\pi^0$) for signals of direct CP-violation was already mentioned by Wolfenstein in [6].

We will see that from the experimental point of view the measurement of slope parameter charge asymmetries is much more stable against systematic errors than f.i. the asymmetries of branching ratios. Moreover, the latter ones are suppressed with respect to the former ones, because the asymmetry of the decay rate is changing its sign with the Dalitz-plot variable Y (see below) and therefore vanishing in first approximation by integrating over Y (from Y_{min} to Y_{max}). An experimental upper limit exists so far only for the $K^{\pm}_{\tau}$ -decay:

$$\Delta g_{\tau} = (-0.7\pm0.5)\cdot10^{-2} \quad [7]$$

From a calculation based on chiral perturbation theory [2], using a procedure where all unknown parameters are fixed by experimental data of K-decays, a relation to $Re(\varepsilon'/\varepsilon)$ - the parameter of direct CP-violation as measured in $K^0_{L,S}$-decays - of the form

$$\Delta g \approx 0.48\cdot Re(\varepsilon'/\varepsilon) \approx 10^{-3} \qquad (1)$$

can be derived. It should be mentioned here, that this prediction is not unquestioned. Recently Cheng [8] argued, that since it disappears in the chiral limit, Δg should be smaller than $\sim 10^{-5}$. Indeed it is determined by symmetry breaking corrections and loop calculations and its model dependence requires further theoretical study. The discrepancy is, however, reduced to one order of magnitude, if the same value of $Re(\varepsilon'/\varepsilon)$ as used in [2], which was taken from experiment [9], is introduced into the estimate of Δg by Cheng, resulting in $\Delta g \approx 10^{-4}$.

The experimental situation for $Re(\varepsilon'/\varepsilon)$ at the given moment (and presumably for the next few years) is not too satisfactory; the latest values have been given by NA31 and E731 [10] as

$$Re(\varepsilon'/\varepsilon) = (2.3\pm0.7)\cdot10^{-3} \text{ and } Re(\varepsilon'/\varepsilon) = (0.6\pm0.7)\cdot10^{-3}$$

resp. Although they are statistically consistent, the central values are mutually excluding each other with >95% confidence.

In this situation we consider it worthwhile to measure $\Delta g_{\tau'}$ with maximal sensitivity, trying to reach the error level corresponding to the error of $Re(\varepsilon'/\varepsilon)$ according to (1). (Due to the larger value of $|g_{\tau'}|$ as compared to $|g_{\tau}|$, the statistical error for $\Delta g_{\tau'}$ is lower than for Δg_{τ}, given the same sample size and measurement accuracy in both cases. There exists no experimental limit for $\Delta g_{\tau'}$ so far.)

Closing this section, we shall repeat for easy reference the standard definitions used here: the slope parameters g, h, k of $K\to3\pi$ decays are defined by the expansion of the squared matrix element in powers of invariant Dalitz-plot variables X, Y

$$|T_{K\to3\pi}|^2 \sim 1 + gY + hY^2 + kX^2 + \ldots$$

where

$$Y = \frac{s_3 - s_0}{m_\pi^2} \quad , \quad X = \frac{s_2 - s_1}{m_\pi^2} \quad , \quad s_i = (p_k - p_i)^2 \quad , \quad s_0 = \frac{1}{3}(s_1 + s_2 + s_3)$$

p_k , p_i - 4-momenta of k^{th} and i^{th} pion. The odd pion has index 3. A term linear in X has to be zero for reasons of symmetry. The (small) parameters h and k are charge symmetric and therefore negligible for CP-violation in $K^{\pm}$-decays.

$$\delta\langle Y\rangle/\delta\theta_{x,y} < 2.5\cdot 10^{-3}/\mathrm{mrad}\ ,\quad \delta\langle Y\rangle/\delta x,y < 0.01/\mathrm{cm}$$

where E, $\theta_{x,y}$ and x,y are energy, divergence and position (at the plane of the anticounter) of the beam.

The monitoring of these parameters performed by reconstructing K momenta from actual decay events does not lead to significant enlargements of the errors compared to those given by the resp. dispersions intrinsic to the beam. From the beam survey [4] these are $\sigma_E \approx 1$GeV, $\sigma_{\theta_{x,y}} \approx 0.7$mrad and $\sigma_{x,y} \approx 2$cm. Therefore, with $\langle Y^2\rangle \approx 0.5$, the conditions (3) are met. Similar considerations could be made for fluctuations in detector efficiencies, which are also being monitored by event samples of size comparable to the complete sample.

All these errors considered so far are independent of the beam polarity. Let us now discuss the error introduced by the cross-section difference between π^+ and π^-, which is of the second type introduced above. The correction of this kind of error requires a M.C. calculation with particular care used in applying the charge dependent $\pi^\pm$ cross-sections for the given energies and materials. This work is in progress. At present we may for a rough estimate of the order of magnitude of these corrections consider the influence of the massive flange, which is part of the end-cap of the decay tube and carries the thin inner window (compare fig.1). It represents about 30g/cm^2 material (Fe and Al) in a ring-shaped region with inner and outer diameter 30cm and 40cm.

After modifying the nuclear interaction length [7] according to charge dependent $\pi^\pm d$ cross-sections at 10 GeV, we find transmission factors 0.71 and 0.74 for π^+ and π^- respectively. From a M.C. calculation, 13.5% of $\pi^\pm$ from all reconstructed $K^\pm_{\tau'}$-decays cross the flange. Therefore we find the variation in efficiency

$$\frac{\Delta\varepsilon}{\varepsilon} = 13.5\%\ \frac{0.74-0.71}{0.74} = 0.55\%$$

The variation in $\langle Y\rangle$ and δg may be maximal of this order of magnitude (the distribution of $\Delta\varepsilon$ over Y is not too different from uniformity). To sum up, we expect corrections of the same order of magnitude as the effect in this case. Therefore it is very

important to have independent cross checks on the (corrected) efficiency.

These consist in comparing lifetime determinations for K^+ and K^- (which should not differ, assuming CPT-invariance) for the $\pi^\pm\pi^0\pi^0$ and the $\pi^\pm\pi^0$ channel, using the decay rates and the decay length distributions. Because very large samples are available, any assumptions used in calculating the efficiency corrections can be cross checked in this way with sufficient accuracy.

IV. Requirements, time schedule

From the physics point of view, the experiment is clearly of great interest, even if one cannot exclude in the present experimental situation that nature conspires in such a way that direct CP-violation is practically invisible in the K sector (our theoretical estimates are based on the experimental results of NA31). Certainly every effort to study this problem in other channels, if it offers chances to reach the required sensitivity, is justified.

We could not find any serious flaw in the conception of the experiment, neither concerning the statistical nor the systematic accuracy, which could speak against its feasibility. The experimental equipment needed for the proposed study is mainly completed now.

We propose the following schedule to perform the experiment:

December 91 run	- 5 days
February 92 run	- 5 days
April 92 run	-15 days
December 92 run	-15 days

and two 30-days runs in 1993-94.

The december 91 and February 92 runs will be used for the final tuning of the detectors and for the measurement of their characteristics. The main goal of the April 92 run is to collect about 10% of the statistics to estimate the real possibilities of the set up to measure $K\to 3\pi$ decays. The other runs are necessary to complete the experiment.

Appendix I. Systematic errors of slope asymmetries

Let us derive the above mentioned functional dependence of g estimates on the effectivity. The likelihood function for g may be written

$$\mathcal{L} = \prod_{i=1}^{N} f(Y_i)$$

where

$$f(Y) = C(1+gY)p(Y)$$

is the probability density for the variable $Y=(s_3-s_0)/m_\pi^2$ to be measured in each event and p(Y) is the effectivity function, including all experimental acceptances as well as the weighting due to the Dalitz-plot X-dependence (quadratic terms as well as contour). Setting

$$\int p(Y)dY = 1$$

and defining moments as

$$\langle Y^n\rangle = \int Y^n p(Y)dY$$

the normalization constant C is

$$C = (1+g\langle Y\rangle)^{-1} .$$

The ML estimate for g (we write also g for simplicity) is to be found from

$$\frac{d}{dg}\ln[\mathcal{L}(g)] = 0 \Rightarrow \frac{1}{N}\sum_i \frac{Y_i}{1+gY_i} = \frac{\langle Y\rangle}{1+g\langle Y\rangle}$$

The functional dependence $\delta g/\delta p$ is given by

$$-\frac{1}{N}\sum_i \frac{Y_i^2}{(1+gY_i)^2}\delta g = \frac{1-\langle Y\rangle^2\cdot\delta g/\delta\langle Y\rangle}{(1+g\langle Y\rangle)^2}\delta\langle Y\rangle$$

The left-hand side is for large N

$$\approx -\int f(Y)\frac{Y^2}{(1+gY)^2}dY\delta g \approx -\frac{1}{1+g\langle Y\rangle}(\langle Y^2\rangle - g\langle Y^3\rangle + g^2\langle Y^4\rangle + \ldots)\delta g$$

This allows the determination of $\delta g/\delta\langle Y\rangle$ as a function of the moments for the distribution p(Y) charge channel. The function $\varphi(\sigma_Y)>1$ reflects the influence of the reconstruction error σ_Y in determining the Dalitz variable Y.

$\varphi(\sigma_Y)$ has been found using an analytical approach, based on the Maximum-Likelihood estimate for g, checking the result by M.C. calculations with σ_Y as input. In tab.1 $\varphi(\sigma_Y)$ and $\sigma_{\Delta g}$ are given for various values of σ_Y.

Tab.1

σ_Y	0	0.1	0.15	0.20
$\varphi(\sigma_Y)$	1.74	1.79	1.87	1.99
$\sigma_{\Delta g}\cdot\sqrt{N}$	1.53	1.58	1.65	1.75

The latter error has been found by reconstruction of Monte-Carlo events, using as an essential input the energy resolution of the e.m. calorimeter as derived from prototype measurements (see sections II, III). Using a kinematical fit with 5 constraints (energy-momentum (4) + π^0-masses (2) - π^+-energy (1)), we get

$$\sigma_Y = 0.176$$

(With unfitted momenta, we have instead $\sigma_Y = 0.189$). For the following estimates we took somewhat pessimistically $\sigma_Y = 0.2$.

In fig.3 the resulting statistical error on Δg is given as function of $N=N(K^+)=N(K^-)$. This can be scaled as well to the effective running time (compare the next chapter on event selection). The corresponding level of sensitivity reached by the K^0 decay experiments [10] for the determination $Re(\varepsilon'/\varepsilon)$ is also given. This shows that the main goal of the experiment, to provide significant alternative information on direct CP violation, can be reached in a reasonable time provided the systematic errors, to be discussed in the chapter III, are under control.

2. Event selection

We shall base the following estimates on the existing version of trigger and DAQ hardware. There is room for further

improvements, however these require more detailed investigation of test data, and should be considered as a reserve.

The general triggering scheme is shown in fig.4. The selection of decaying $K^\pm$ with the help of 5 beam counters chosen from $S_1 \ldots S_8$, with the last one, placed after the decay tube, in anti coincidence, is performed by scintillation counter logic SI, followed by the Cerenkov logic DC, which evaluates up to 4 threshold Cerenkov signals and up to 8 Differential Cerenkov conditions.

After this 1^{th} level trigger, we expect a maximum rate of $5\cdot10^4$ K-decays/burst (for a beam intensity of 10^7 particles/burst, with the K-content of 2.5%, and with 20% decaying inside of the decay tube). Out of these, 1.73% (865 decays) belong to the investigated channel $K^+\to\pi^+\pi^0\pi^0$ (see fig. 5).

At the 2^{nd} level, the analog information from the e.m. calorimeter is used by the total sum trigger unit TL to select events with enhanced shower activity. In the given case the total sum, being proportional to the total energy release in the detector, is broken down into 16 partial sums (4 for each quadrant), which have to pass given thresholds (1-2 GeV). The total number of signals is required to be ≥ 3 (Actually, the 16 discriminator outputs are evaluated with a look-up table, allowing the introduction of further conditions, e.g. at least two quadrants with large signals).

According to M.C. studies, we find the suppression factors 50%, 14% and 10% for the channels $\pi^\pm\pi^0\pi^0$, $\pi^0e^\pm\nu$ and $\pi^\pm\pi^0$ resp. Other decay channels are practically completely suppressed. The maximum trigger rate would then be $1.8\cdot10^3$ selected K-decays/burst. After combining it with possible further trigger conditions (Additional trigger unit EX and Final trigger unit FT) this trigger starts the read-out of the ADC's from the e.m. calorimeter and of the digital decay registers (DD's) from the large hodoscopes.

The ADC read-out, together with pedestal subtraction and zero suppression, requires 1.5 μs/channel. The readout is made in parallel for the 4 quadrants and serially for the 500 channels in each quadrant, resulting in 750 μs/event. So the maximum rate is $1.3\cdot10^3$ events/burst (with a spill length of 1s). Only with 1.5s spill the maximal rate of $1.8\cdot10^3$ will be reached. For the "normal" speed $1.3\cdot10^3$ events/burst, the number of accepted $\pi^+\pi^0\pi^0$ events would be ~300/burst, with an S/B ratio of 1:3.

After buffering, these data, together with the hodoscope and beam information, are written on tape, using the time of 7s until the next burst. A further selection by means of a fast processor based on transputers has been considered; it could reduce the amount of data by a factor 2 and would therefore be helpful for the further off-line data handling.

Finally, the rate of reconstructed events out of those triggered is expected from M.C. to be 23%. All this results then in $7\cdot10^5$ good events per day of effective data taking ($=10^4$ bursts). This is the basis for fig.3.

3. Systematic errors

The systematic errors of charge asymmetries of the Dalitz plot slope are of two kinds:

1. Those resulting from changes either in beam- or in detector conditions from run to run, not directly dependent on beam polarity,
2. Polarity dependent systematic errors, most importantly those connected to cross-section differences between π^+ and π^-.

Whereas the former ones produce spurious slope asymmetries between different runs, which have to be controlled and corrected for, they would diminish only the statistical accuracy of the experiment, insofar as their effect does not depend on the beam polarity. We will show that the errors remaining after correcting these effects, are proportional to $1/\sqrt{N}$ where N is the sample size as in the case of statistical errors. To the extent that they can be kept small compared to the statistical errors in each individual run, they do not matter. As far as the second kind of errors is concerned, this condition would be not sufficient, because the corrections to be applied now depend on the polarity of the beam and so may the residual errors. In this case the latter ones have to be kept small compared to the overall statistical error.

Any kind of systematic change influences the slope g exclusively via the efficiency distribution with resp. to Y. In the appendix, the relation:

$$\delta g \approx -\frac{1}{\langle Y^2\rangle}\,\delta\langle Y\rangle \qquad (2)$$

is derived, where $\langle Y\rangle\approx0.2$, $\langle Y^2\rangle\approx0.5$ are the first and second moments of the distribution p(Y), which is the phase-space distribution for Y, multiplied with the efficiency distribution. If the latter would be flat, there could not be any variation $\delta\langle Y\rangle$ of the first moment and g would be completely stable. The (preliminary) efficiency distribution expected from M.C. calculation for our set-up is given in fig.6. It is important that it is rather flat in the region Y<0, allowing to cut down systematic errors by restricting the Y-range, loosing of course statistical accuracy for g. The decrease for large Y is due to the anticounter, cutting out the beam region together with small angle charged pions (for large Y, the invariant mass $s_3=(p_1+p_2)^2$ of the two neutral pions is large, leaving less CMS-momentum, therefore also less transverse momentum, to the charged one).

First we discuss the errors of the first kind. In order to find the necessary corrections δg, one has to determine by M.C. the quotients $\delta\langle Y\rangle/\delta E$, where E is, e.g., the mean beam energy or any other parameter that may change, and to relate δg to δE by (2). The residual error is given by the accuracy with which δE is determined, which in turn depends on N, the statistics taken for monitoring of E, and σ_E, the dispersion of E:

$$\sigma(\delta E) = \sigma_E/\sqrt{N}$$

Assuming N to be the same as that for estimating g, we find the condition (compare (1) and section 1))

$$\frac{1}{\langle Y^2\rangle}\,\frac{\delta\langle Y\rangle}{\delta E}\,\sigma_E << 1 < \varphi(\sigma_Y) \qquad (3)$$

For the case of beam parameters, the following quotients have been determined by M.C. calculations:

$$\delta\langle Y\rangle/\delta E = 0.01/\mathrm{GeV}\ ,$$

The asymmetry between the slope parameters g^+ and g^- can be characterized by:

$$\Delta g = \frac{g_{K^+} - g_{K^-}}{g_{K^+} + g_{K^-}}$$

II. Experimental Set-Up

The experimental set-up consists of a minimum configuration of the Tagging Neutrino Facility which is described in the appendix (see fig.1 for a general view). The intensity of the secondary hadron beam [4] to be used for this experiment will be up to 10^7 particles/burst (flat top 1-2 sec, 400 bursts/h), two orders of magnitude less than the maximal one. The beam polarity can be reversed. The beam momentum is measured to an accuracy of 2%.

$K^\pm$ decays inside of the evacuated decay tube of 58.5 m length are selected by means of an vetocounter at it's exit. At 35 GeV about 22% of the $K^\pm$ will decay within the tube. For the measured K-content of 2-3% we expect $5\cdot10^4$ decays/burst.

The particles from the decay $K^\pm \to \pi^\pm\pi^0\pi^0$ are detected using 3 scintillator hodoscopes, each measuring 2 perpendicular coordinates x,y in the transversal plane and the electromagnetic calorimeter "GEPARD", measuring the 4 γ's . The relevant details of the detectors are found in the appendix.

In the following we describe the actual status of hard- and software.

1. Beam.

Slow ejected 70 GeV protons are transported from the IHEP accelerator to the target using beam channel N8. Two dipoles and seven quadrupoles downstream from the target form the beam channel N23 to select secondaries in the momentum range of 10 to 35 GeV/c ($\Delta p/p$ can be changed from 1.6% to 8.0%) and to make a parallel beam (σ_θ is about 0.5mrad) at the end. The length of the beam channel N23 is 60m, the secondary beam intensity is 10^6-10^{10} for

the positive particles and 10^5-10^9 for the negative ones (per cycle).

The beam layout is shown schematically in fig.2. Four scintillation beam counters and four (x-y) scintillation hodoscopes with 5mm logic elements are used to measure the particle flux, beam position and particle directions at the entrance window of decay pipe. Particle identification is performed with 3 threshold and 2 differential Cerenkov counters. The background level at the kaon peak is less than 1% for both K^+ and K^- at 35 GeV.

2. Decay tube

The 58.5m decay tube is kept at a pressure of 10^{-4} atm. The end flange is made of 4mm steel with an inner window of 2mm aluminum. This leads to the following complications for the experiment:

1. The frequent photon conversions in the 4mm steel flange make the track finding procedure in the hodoscopes more difficult.
2. The energy resolution in the e.m.-calorimeter is somewhat degraded.
3. The trigger rates from the unwanted decays into $\pi^\pm\pi^0$ and $\pi^0e^\pm\nu$ are raised due to asymmetric pair production.

However MC investigations show, that the problems are manageable, as will be shown below.

3. Hodoscopes

Six planes (3x,3y) of scintillation hodoscopes are used to measure the charge particle trajectory. An additional pair of x,y planes, not shown in fig.1, is placed behind the e.m.calorimeter and an additional 3m steel absorber to identify muons. The width of scintillation strips in each hodoscope is 14mm. The outer dimension of hodoscopes is about 4m. All hodoscopes have a beam hole of diameter 20cm. A geodesic survey has been made for all the detectors. Further technical details are given in [14].

4. E. M. calorimeter GEPARD-2000.

The Calorimeter consists of 1968 cells. Each cell has 40 scintillator and 40 lead interleaved layers with thickness of 5mm(Sc) and 3mm (Pb). The cell size is 76x76mm. 2mm thick WLS are used to collect the scintillation light onto FEU-84-3 PM. The energy resolution measured with a 26 GeV electron beam is 6% (FWHM), the maximum nonuniformity is 3%, the spatial resolution is $14\text{mm}/\sqrt{E}$ [15].

The absolute calibration (see appendix III) of the GEPARD is made with 10 GeV e^- swept by two magnets across the surface of the detector. For continuous monitoring of the cell sensitivity a LED system is used.

Zero signal suppression and pedestal subtraction are realized by the front end electronics. From the first test data it follows that the zero signal suppression leaves on average of about 20 noise channels per event. This complicates somewhat the recognition of minimum ionizing particles. Especially the number of m.i.p. cannot be used as a trigger criterion. We expect a better adjustment of some channels.

5. Electronics and data acquisition

All parts of the electronics needed for a first data taking are working. This includes, besides front-end electronics, all digital delay registers for the large hodoscopes (4096 channels) as well as digital and analog read-out channels for the e.m. calorimeter. A higher level trigger, derived from the analog sums of 12 adjacent calorimeter cells, is completed and integrated into the overall trigger scheme (see section III,2). The same is true for the track-finder electronics of the large hodoscopes [11]

All detectors are served by microcomputers of LSI-11 type (2 for the beam equipment, 3 for the large hodoscopes, 4 for the e.m. calorimeter). The links are provided by a local area network (IRONET) [12], which also transfers the data to the central minicomputer. The tape records are of a very compressed form (about 200 bytes/event).

The electronic equipment was developed with the main goal of maximum rate capability and data compression. It uses mainly Eurostandard and ECL technology. All parts are designed, build and maintained by the Serpukhov group. This development, now being completed, has to a large extent set the time scale for the completion of the whole experimental set-up.

6. Software

M.C. calculations were done mainly with the help of the CATAS code [13] supplying it with adequate event generators and analyzing routines (geometrical and kinematical fit). The results, especially concerning shower development, have been compared also with GEANT-generated data.

Since the last year a more systematic reconstruction and analyzing program, TITAN, is under work. GKS based graphics is foreseen. The present tasks are adaptation of existing analysis code, providing some interface routines and further development of filtering and track matching programs, correction of relative positions of the hodoscope planes and the connection to the beam hodoscopes by means of the determination of the best fitting beam axis with the help of test data. Data exchange on tape has been accomplished.

III. Statistical and systematical errors, sensitivity of the experiment

1. Statistical error

The statistical error of the slope parameter asymmetry, $\sigma_{\Delta g}$ is given as

$$\sigma_{\Delta g} = \frac{1}{\sqrt{2}} \cdot \frac{\sigma_g}{g}$$

where

$$\sigma_g/g = \varphi(\sigma_Y)/\sqrt{N}$$

is the error for estimating the slope g from N events in each

$$\frac{\delta g}{\delta\langle Y\rangle} = \frac{-1}{(1+g\langle Y\rangle)(\langle Y^2\rangle - g\langle Y^3\rangle + g^2\langle Y^4\rangle + \ldots) - \langle Y\rangle^2} \approx -\frac{1}{\langle Y^2\rangle},$$

to a very rough approximation, neglecting any odd and higher moments; we found by MC $\langle Y\rangle = -0.2$ and $\langle Y^2\rangle \approx 0.5$. $\delta\langle Y\rangle$ should not be confused with the usual statistical error

$$\delta\langle Y\rangle_{stat} \approx \left(\frac{1}{N}\langle Y^2\rangle\right)^{1/2}$$

but is defined as the systematic deviation of the mean value due to shifts in the p-distribution caused by asymmetries in experimental conditions between K^+ and K^- runs.

Appendix II. Technical setup

<u>Detector:</u> Scintillation hodoscopes of the tagging station
Name: Scintillator hodoscopes
Function: Measurement of the parameters of the trajectory of charged particles in the tagging station
Z-coordinates of the detectors 1. 61 m
2. 64 m
3. 67 m
Shape: Octogonal
Modules: 2 planes
Coord.: measures X,Y
Length: mechanical : 1060 mm
Width: mechanical : 4080 mm
Height: mechanical : 4080 mm
Channels: 1024

<u>Modules:</u>
Elements: 512
Shape: plane, octogonal
Channels: 512
Width: mechanical : 4080 mm , active : max 3584 mm
Height: mechanical : 4080 mm , active : max 3584 mm
Thickn.: mechanical : 530 mm , active : 12 mm

<u>Elements:</u>
Measured
Values: logical signal of scintillation light amplitude
Shape: rod with rectangular section
Length: active : max 1916 mm
Width: mechanical : 14 mm , active : 14 mm
Thickn.: mechanical : 12 mm , active : 12 mm
Channels: 1 (FEU 84)
Material: PMMA + 3% Naphtaline + 1% PPO + 0.1% POPOP
Radiat.Length: 0.0356 L_R
Interact.Length: 0.0172 λ_I
Density: 1.2 g/cm^3
Remarks: yield of photoelectrons > 11/(min. ioniz. particle)

attenuation length of scint. light : 1.4...1.5 m
emission maximum of the scintillator : 415 nm
scintillation lifetime : 4.5 ns
critical radiation dose (rad. damage) : 2 Mrad

Detector: Electromagnetic Total Absorption Spectrometer (TAS)
Name: GEPARD-2000
Function: Measurement of energy and coordinates of $e^{\pm}$ and γ
Shape: Octogonal
Modules: 1968 (48x48 without corners)
Elements: 40x1968 = 78720
Coord.: measures X and Y
Length: 2m (mechanical length)
Width: 4.5m (mechanical width)
Height: 4.5m (mechanical height)
Channels: 24x24x4 ADC ,

Modules:
Elements: 40
Shapes: quadratic
Width: active: 76 mm
Height: active: 76 mm
Thickn.: active: 320 mm ; mechanical: 700 mm
Struct.: 40x(5mm scintillator Polystrene + 3mm Pb)
Radiat.length: 20 L_R
Interact.length: 1 λ_I
Remarks: energy resolution $\sigma_E/E \sim 0.15/\sqrt{E}$/GeV
critical radiation dose (rad. damage) 10^7 rad

Appendix III. Calibration of E.M. Calorimeter

For the purpose of calibration, the negative beam has been set at 10 GeV/c and the trigger derived from beam counters and Ç-counters in such a way, as to select electrons. By means of an additional magnet (which is removed for usual data taking), the beam can be swept cross the detector surface. At the same time, it cannot be defined to a small area, and it would require a small additional trigger counter (or hodoscope) in front of the shower detector to select events with just one cell hit. The calibration procedure was the following:

Let A_{ij} be the amplitude (ADC-signal after pedestal subtraction) seen in channel i for the event j. After division by the coefficient α_i (which is to be determine) it should be represent some (unknown) fraction A_{ij}/α_i of the total energy (here 10 GeV).

Starting with some 0^{th} approximation α_i^0, we calculate successively (for $j=1,\ldots,N_{ev}$)

$$\alpha_i^{(j)} = \alpha_i^{(j-1)}\left[1 + \left(\sum_k \frac{A_{kj}}{\alpha_k^{(j-1)}} - 1\right)\cdot\omega_{ij}\right], \quad i=1,\ldots,N_{ch}$$

As weights ω_{ij} we chose

$$\omega_{ij} = A_{ij}^2 / \sum_k A_{ik}^2$$

The results do not depend significantly from the sequence of events and the start values chosen. The weights have to enhance events, where the given channel received large signals, their exact form is not important.

In case of channels at the edge of the detector, one has to demand, that signals are seen on inner neighboring channels as well, in order to avoid leakage of energy.

Comparison with results from exact minimization (for some part of the detector) and M.C. simulation showed, that the remaining error (after taking not less than 100 events/channel) is of the order of 5%.

Figure captions

fig.1 Set-up for K-decay experiment

fig.2 Beam part

$M_{1,2}$ analyzing, compensating magnet $C_{1,2}$ correction magnets;
$Q_{1..7}$ quadrupoles; $K_{x,y}$ horizontal, vertical collimators;
$C_{1..3}$ threshold -counters; $DC_{1,2}$ differential -counters;
$S_{1..8}$ scintillation counters; $H_{1..4}$ beam hodoscopes;
T proton target

fig.3 Statistical error of slope asymmetry Δg

fig.4 Trigger control system

fig.5 Data selection for $K^{\pm} \longrightarrow \pi^{\pm}\pi^{0}\pi^{0}$

fig.6 Preliminary efficiency distribution
(due to limited M.C. statistiscs)

References

[1] V.V.Ammosov et al., Experiments with tagged neutrino beam at IHEP accelerator, Proposal SERP-E-152, (1984)
[2] A.A.Bel'kov et al., Phys. Lett. B232 (1989) p.118
[3] Collaboration " Neutrino Tagging" PHE 90-07
[4] M.V Akopyan et al., Internal material of TNF-collaboration
[5] L.Wolfenstein, Phys. Rev. Lett. 13 (1964), p.562
[6] L.Wolfenstein "Theory and Phenomenology in Particle Physics" Ed. A.Zichichi, Academic Press, New York, London, (1969)
[7] Particle data Group, Phys. Lett. B239, (1990)
[8] H.Y.Cheng, Contr. to Europhys. Conf. HEP, Geneva, (1991)
[9] H.Burkhardt et al., preprint LAL 88-36, Orsay 1988, p.55
[10] G.Barr, B.Winstein, Parallel session, Europhys. Conf. HEP, Geneva, (1991)
[11] A.V.Kozelov et al., Serpukhov IFVE 90-139 (russ.)
[12] A.V.Kozelov et al., Serpukhov IHEP 88-50
[13] A.S.Vovenko et al., NIM 212, p.155, (1983)
[14] J.Bähr et al.,Serpukhov IFVE 91-61 (russ.)
[15] V.M.Buyanov et al.,Serpukhov IFVE 89-45 (russ.)

EXPERIMENTAL SETUP : $K^{\pm} \rightarrow \pi^{\pm}\pi^{0}\pi^{0}$

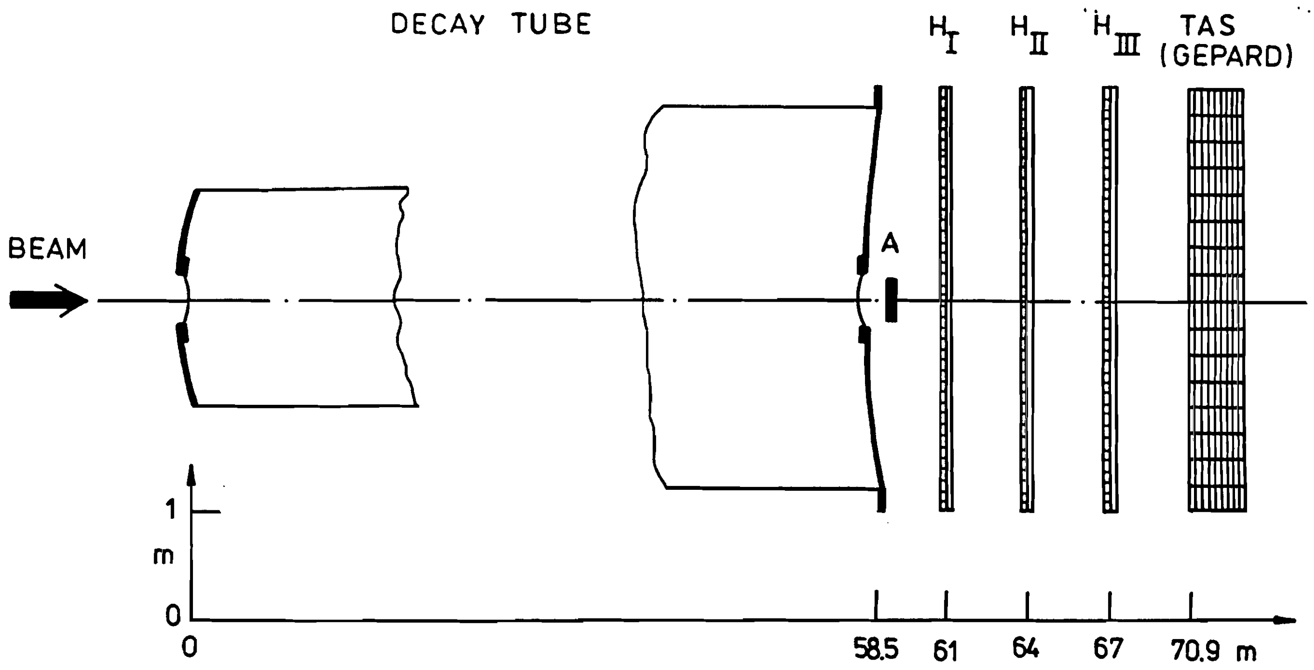

Fig. 1

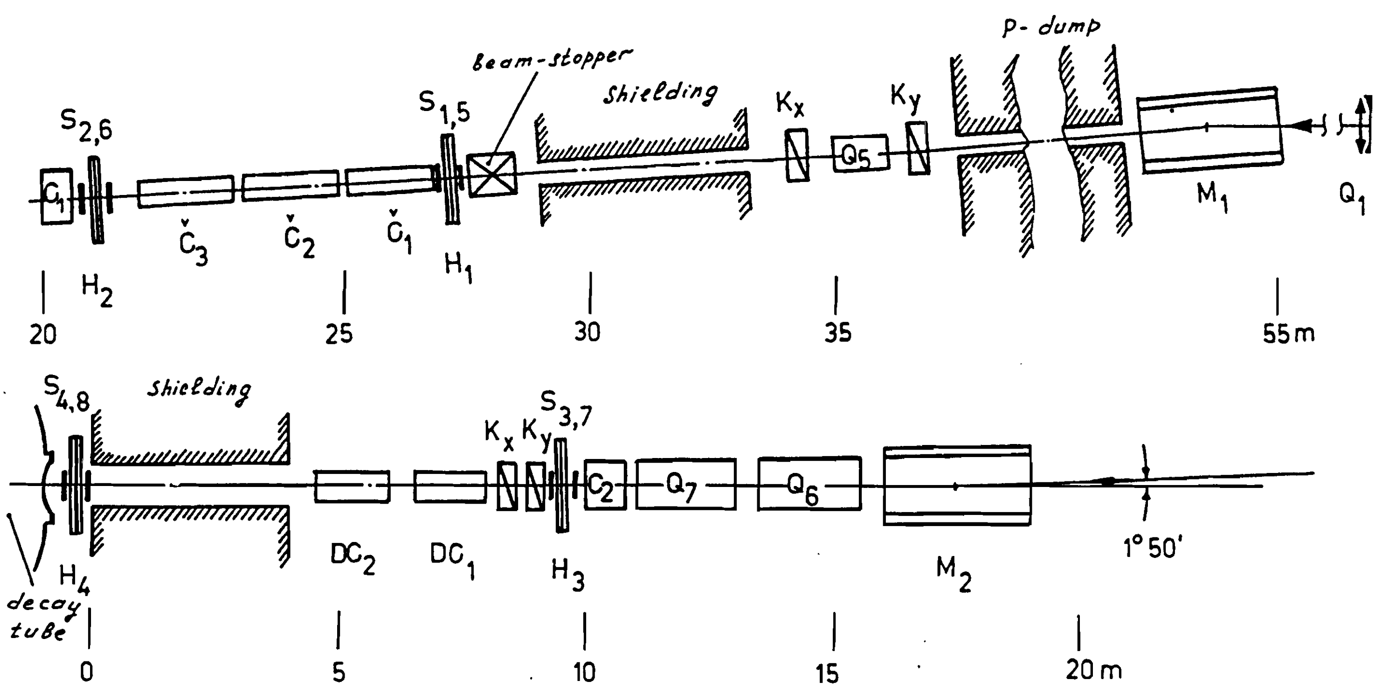

Fig. 2

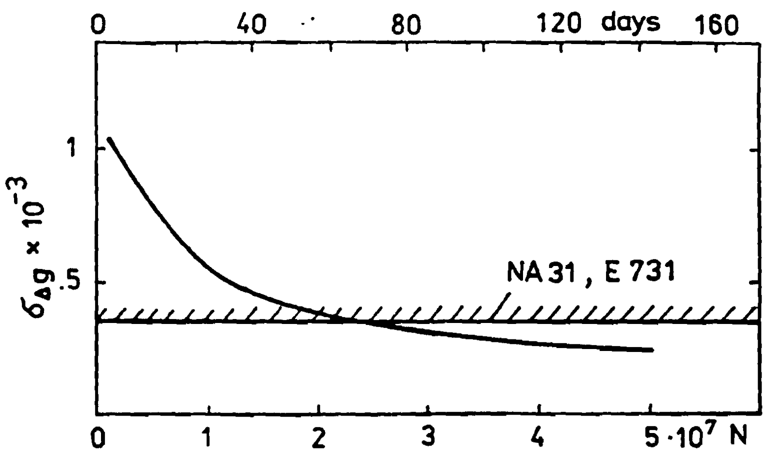

Statistical error of Δg

Fig.3

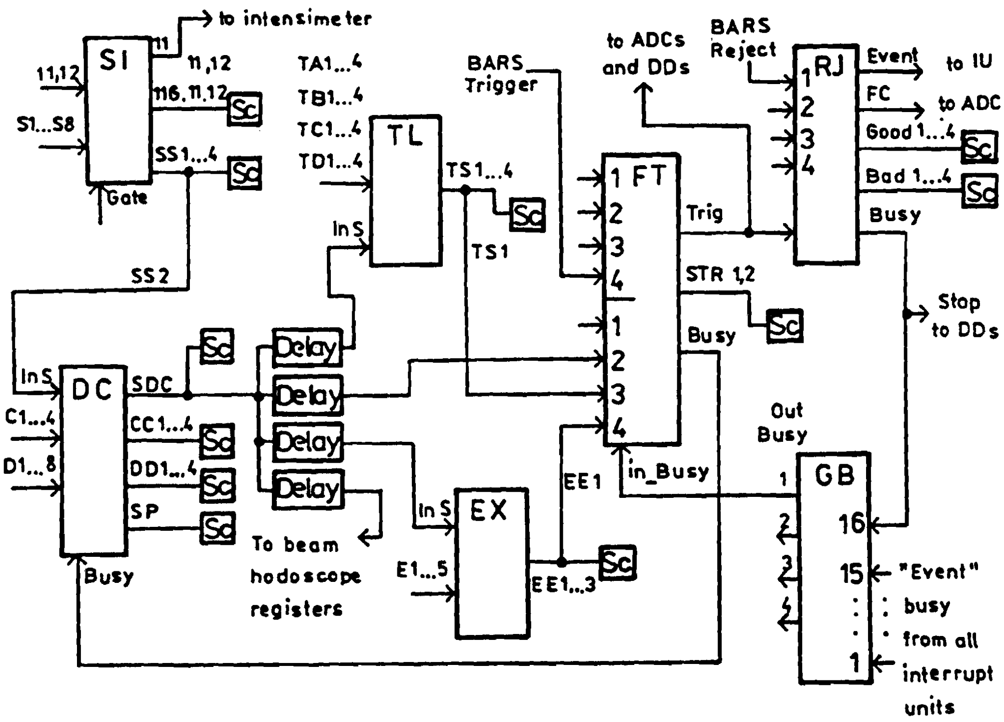

TNF trigger control

Fig.4

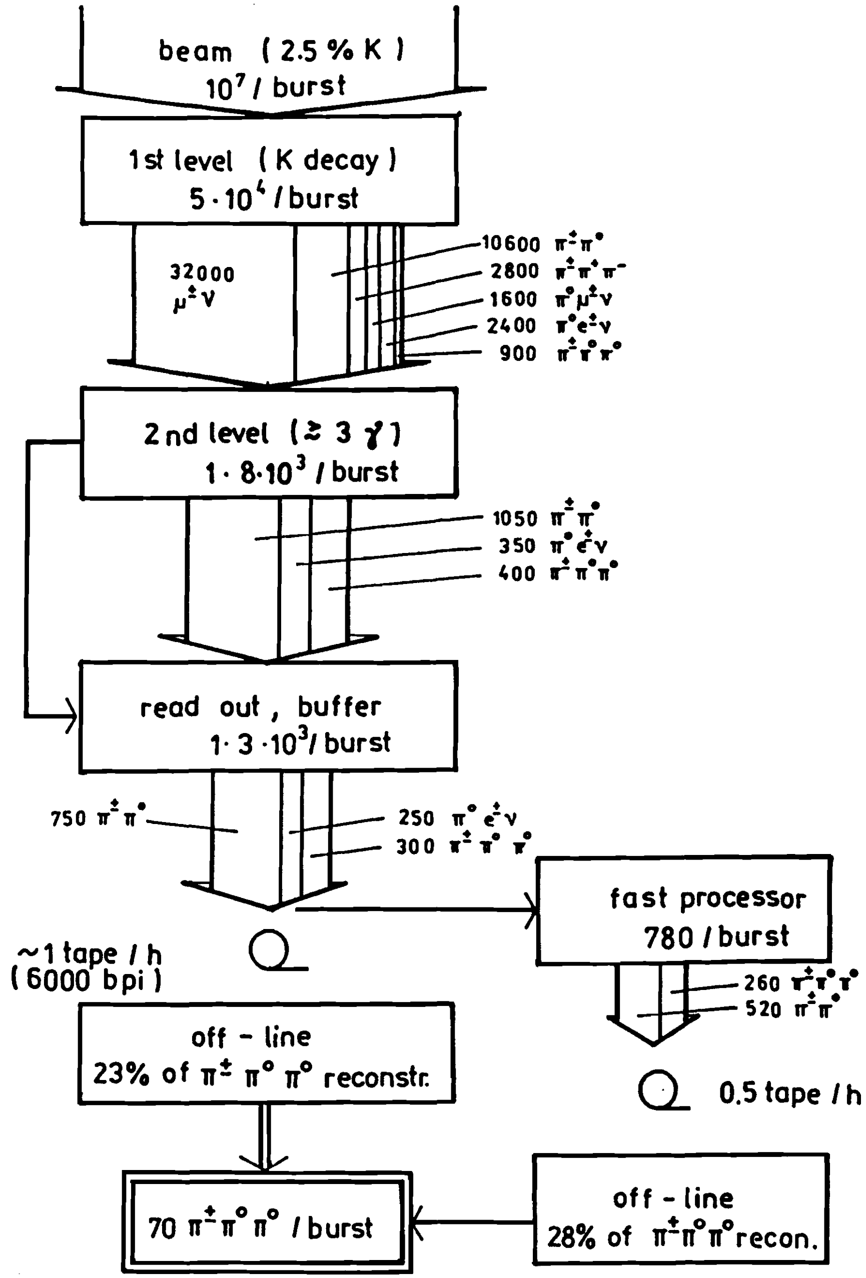

Event selection

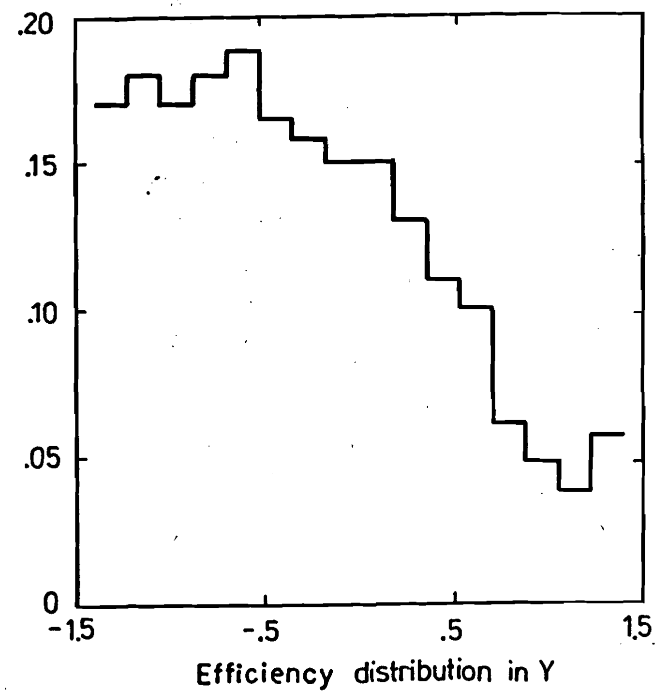

Fig.6

Words cut off on original paper copy.